Dynamical Quantum Phase Transitions: Role of Topological Nodes in Wave Function Overlaps

Zhoushen Huang[1,*] and Alexander V. Balatsky[1,2,†]
[1]*Institute for Materials Science, Los Alamos National Laboratory, Los Alamos, New Mexico 87545, USA*
[2]*NORDITA, Roslagstullsbacken 23, SE-106 91 Stockholm, Sweden*
(Received 15 April 2016; published 15 August 2016)

A sudden quantum quench of a Bloch band from one topological phase toward another has been shown to exhibit an intimate connection with the notion of a dynamical quantum phase transition (DQPT), where the returning probability of the quenched state to the initial state—i.e., the Loschmidt echo—vanishes at critical times $\{t^*\}$. Analytical results to date are limited to two-band models, leaving the exact relation between topology and DQPT unclear. In this Letter, we show that, for a general multiband system, a robust DQPT relies on the existence of nodes (i.e., zeros) in the wave function overlap between the initial band and the postquench energy eigenstates. These nodes are topologically protected if the two participating wave functions have distinctive topological indices. We demonstrate these ideas in detail for both one and two spatial dimensions using a three-band generalized Hofstadter model. We also discuss possible experimental observations.

DOI: 10.1103/PhysRevLett.117.086802

Introduction.—Advances in experimental techniques, particularly in cold atom systems [1–3], have reinvigorated recent interest in quantum dynamics [4]. A paradigmatic setup in this context is a quantum quench [5–9], wherein a system is prepared as an eigenstate $|\Psi\rangle$ of an initial Hamiltonian H_I but evolved under a different Hamiltonian H_F. In a slow ramp [10,11], one has, in addition, control over how fast the switching between H_I and H_F can be, as well as what path to take in the space of Hamiltonians. Since $|\Psi\rangle$ typically consists of many excited states of H_F with a nonthermal distribution, its time evolution provides a unique venue for investigating issues in nonequilibrium quantum statistical mechanics such as thermalization, equilibration, and the lack thereof [4,12–16]. A particularly fruitful approach to understanding dynamics after a quantum quench is by exploiting the formal similarity between the time evolution operator $\exp(-iHt)$, and the thermal density operator $\exp(-\beta H)$. This enables one to leverage and extend notions in equilibrium statistical mechanics to the realm of quantum dynamics. In this spirit, the return amplitude

$$G(t) = \langle\Psi|e^{-iH_F t}|\Psi\rangle = \sum_n |\langle\Phi^{(n)}|\Psi\rangle|^2 e^{-iE_n t} \qquad (1)$$

can be thought of as a partition function along imaginary temperature $\beta = it$, with the prepared state $|\Psi\rangle$ as a fixed boundary [17]. Here, $|\Phi^{(n)}\rangle$ and E_n are eigenstates and eigenvalues of the postquench H_F, respectively. Heyl *et al.* showed [18] that, analogous to the thermal free energy, a dynamical free energy density [19] can be defined, $f(t) = -\log G(t)/L$, where L is the system size. Singularities in f then signifies the onset of what was proposed as a *dynamical quantum phase transition* (DQPT). In statistical mechanics, phase transitions are closely related to the zeros of the partition function—known as Fisher zeros—in the complex temperature plane [20]. Historically, Yang and Lee were the first to connect phase transitions with zeros of the partition function in complexified parameter space [21]. While Fisher zeros are always complex for finite systems, they may coalesce into a continuum (a line in one parameter dimension, area in two parameter dimensions, etc.) that cuts through the real temperature axis in the thermodynamic limit, giving rise to an equilibrium phase transition. Investigations on DQPTs have followed a similar route by first solving the Fisher zeros in the complex temperature plane, and then identifying conditions for them to cross the axis of imaginary temperature (real time). A DQPT is thus mathematically identified as $G(t^*) = 0$ at critical time(s) t^* [22]. DQPTs occur in both integrable [18,23–30] and nonintegrable [19,31–34] spin systems for quenches across quantum critical points. They can further be classified by discontinuities in different orders of time derivatives of $f(t)$ [27,35] *vis-à-vis* their thermal counterparts. Very recently, DQPTs have also been shown to constitute *unstable* fixed points in the renormalization group flow, and they are therefore subject to the notion of universality class and scaling [36].

Physically, the return amplitude $G(t)$ is related to the power spectrum of work performed during a quench, $G(\omega) = \sum_n |\langle\Phi^{(n)}|\Psi\rangle|^2 \delta(\omega - (E_n - E_I))$, which is the Fourier transform of $G(t)e^{-iE_I t}$, and E_I is the energy of the initial state [37–40]. This, in principle, makes $G(t)$—and hence the DQPT—a measurable phenomenon. A practically more viable route to experimental verification is through measuring time evolution of thermodynamic quantities, which may exhibit postquench oscillations at a time scale commensurate with the DQPT critical time t^*, and universal scaling near t^* [41]. In band systems, as we will show, they may also be identified by a complete depletion at t^* of the sublattice or the spin-polarized particle density at certain crystal momenta; see Eq. (8).

Parallel to the development of DQPTs as the dynamical analogue of equilibrium phase transitions is the investigation on its relation with topology [24–27]. This issue arises naturally because, in the transverse field Ising model, in which DQPT was first discovered, the quantum critical point can be mapped to a topological phase transition at which the quantized Berry phase of the *fermionized* Hamiltonian jumps between 0 and π. The DQPT in this two-band fermion model was attributed to the occurrence of "population inversion," [18] where it becomes equally probable to find the initial state in either of the two postquench bands, a consequence of the Berry phase jump [26]. The same analysis has been extended to various two-band models in one- (1D) and two-spatial dimensions (2D) [25–29], where a definitive connection was found between the DQPT and the quench across topological transitions, although some complications exist [42]. DQPTs have also been demonstrated to occur for quenches within the same topological phase [24,25,33], although, from the point of view of topological protection, these are not robust, as they require fine-tuning of the Hamiltonians.

The purpose of this Letter is to develop a general theory *beyond two band models* to clarify the relation between a *robust* DQPT and topology. We will show that a robust DQPT—one which is insensitive to the details of the pre- and postquench Hamiltonians other than the phases to which they belong—relies on the existence of zeros (or nodes) in the wave function overlap between the initial band and all eigenstates of the postquench Hamiltonian. These nodes are topologically protected if the two participating wave functions have distinctive topological indices: for example, the Chern number difference $|C_\psi - C_\phi|$ provides a lower bound to the number of $\boldsymbol{k}$-space nodes in the overlap $\langle\phi_{\boldsymbol{k}}|\psi_{\boldsymbol{k}}\rangle$; see Theorem 1. These considerations lead to the notion of *topological* and *symmetry-protected DQPTs*, which we will demonstrate in detail using a three-band generalized Hofstadter model. Analysis of a 1D three-band model exhibiting a symmetry-protected DQPT can be found in the Supplemental Material (SM) [43].

Amplitude and phase conditions of the DQPT.—The DQPT condition $G(t^*) = 0$ can be interpreted geometrically as the complex numbers $z_n(t) = |\langle\Phi^{(n)}|\Psi\rangle|^2 e^{-iE_n t}$ forming a closed polygon in the complex plane at t^*; see Fig. 1. The time-independent content of this observation is that the amplitudes $\{|z_n|\}$ satisfy a generalized triangle inequality, $\sum_{m\neq n}|z_m| \geq |z_n|\ \forall n$. Invoking $\langle\Psi|\Psi\rangle = \sum_n |z_n| = 1$, one has the *amplitude condition*,

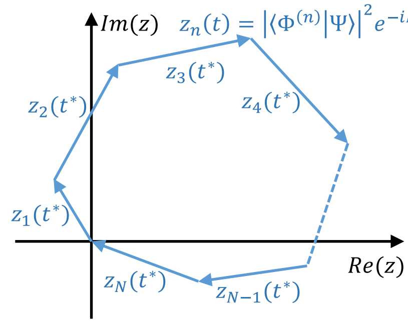

FIG. 1. Geometric representation of the DQPT condition $G(t^*) = \sum_n z_n(t^*) = 0$. $\{z_n(t^*)\}$ must form a closed polygon in the complex plane and would hence satisfy a generalized triangle inequality $|z_n| \leq \sum_{m\neq n}|z_m|$. Wave function normalization $\langle\Psi|\Psi\rangle = \sum_n |z_n| = 1$ then leads to $|z_n| \leq \frac{1}{2}$.

$$|z_n| = |\langle\Phi^{(n)}|\Psi\rangle|^2 \overset{!}{\leq} \frac{1}{2} \quad \forall n. \tag{2}$$

For $\{|z_n|\}$'s that satisfy Eq. (2), solutions to $\sum_n |z_n| e^{-i\varphi_n} = 0$ exist and form a subspace $\mathcal{M}_{\{|z_n|\}}$ on the N-torus,

$$\mathcal{M}_{\{|z_n|\}} \in \mathcal{T}^N : \left\{ \{e^{-i\varphi_n}\} \middle| \sum_{n=1}^{N} |z_n| e^{-i\varphi_n} = 0 \right\}. \tag{3}$$

To set off a DQPT, the dynamical phases must be able to evolve into $\mathcal{M}_{\{|z_n|\}}$. This constitutes the *phase condition*,

$$\exists t^* : \{e^{-iE_n t^*}\} \in \mathcal{M}_{\{|z_n|\}}. \tag{4}$$

The DQPT requires both conditions to hold simultaneously.

Phase ergodicity in few-level systems.—At first glance, the phase condition may seem to be the more stringent one. After a quench across a quantum phase transition, a many-body initial state $|\Psi\rangle$ typically has an overlap with an extensive amount of eigenstates of the postquench Hamiltonian H_F, and the amplitudes $\langle\Phi^{(n)}|\Psi\rangle$ are therefore generically exponentially small in system size, rendering Eq. (2) satisfied in general. Existence of a DQPT then relies entirely on the phase condition. Integrable systems, however, point to the possibility that the amplitude and the phase conditions may be intricately related and traded for one another. Such systems can effectively be broken down into few-level subsystems labeled by quantum numbers $\boldsymbol{k}$, say, $N_{\boldsymbol{k}}$ levels $\{E_{\boldsymbol{k},n}\}$ for $n = 1, 2, \ldots, N_{\boldsymbol{k}}$ in the $\boldsymbol{k}$ sector. Correspondingly, $G(t) = \prod_{\boldsymbol{k}} G(\boldsymbol{k}, t)$. For the transverse field Ising model, Kitaev's honeycomb model [44], and band insulator models, $\boldsymbol{k}$ is the Bloch momentum. It is known that as long as the $N_{\boldsymbol{k}} - 1$ gaps, $\Delta_{\boldsymbol{k},n} = E_{\boldsymbol{k},n+1} - E_{\boldsymbol{k},n}$, are not rationally related, the dynamical phases $\{e^{-iE_{\boldsymbol{k},n}t}\}$ are *ergodic* on the $N_{\boldsymbol{k}}$-torus up to an overall phase [45], and *will* therefore evolve into its subspace $\mathcal{M}_{\{|z_n|\}}$ [Eq. (3)]. Phase ergodicity thus guarantees the phase condition equation (4), and the DQPT in each $\boldsymbol{k}$ sector depends entirely on the amplitude condition.

Robust DQPT protected by nodes in wave function overlap.—Hereafter, we focus on quenches in multiband Bloch systems with N_B bands. For simplicity, we use a single filled band $|\psi(\boldsymbol{k})\rangle$ as the prequench state. Generalization to multiple filled bands is straightforward. The postquench return amplitude is $G(t)=\prod_{\boldsymbol{k}}G(\boldsymbol{k},t)$,

$$G(\boldsymbol{k},t)=\sum_{n=1}^{N_B}|\langle\phi^{(n)}(\boldsymbol{k})|\psi(\boldsymbol{k})\rangle|^2 e^{-i\epsilon_n(\boldsymbol{k})t}, \tag{5}$$

where $|\phi^{(n)}(\boldsymbol{k})\rangle$ and $\epsilon_n(\boldsymbol{k})$ are, respectively, the postquench energy eigenstates and eigenvalues. Assume phase ergodicity holds at all $\boldsymbol{k}$ points—this is a very relaxed requirement provided that there is no degeneracy at any $\boldsymbol{k}$ point. Then the DQPT amounts to the existence of at least one $\boldsymbol{k}$ at which Eq. (2) is satisfied, namely,

$$\exists\boldsymbol{k}\in\text{Brillouin zone}:|\langle\phi^{(n)}(\boldsymbol{k})|\psi(\boldsymbol{k})\rangle|^2\leq\frac{1}{2}\quad\forall n. \tag{6}$$

We now discuss how Eq. (6)—and hence the DQPT—can arise from nodes in wave function overlaps. Note that this is *not* the only way to get a DQPT. Its virtue lies in its robustness against perturbations to the Hamiltonians. In the SM [43], we provide examples where DQPTs with no overlap node can be easily avoided simply by Hamiltonian parameter tuning without crossing a phase boundary. The overlap nodes are, on the other hand, typically topologically protected, a point that we will return to later. Now consider the following quench. Let $a=1,2,\ldots,N_B$ label "sublattices," which, in general, may also include other degrees of freedom, e.g., orbitals, spins, etc. Prepare the prequench state by filling $a=1$,

$$|\Psi\rangle=\prod_{\boldsymbol{r}}\psi^\dagger_{\boldsymbol{r},1}|\emptyset\rangle=\prod_{\boldsymbol{k}}\psi^\dagger_{\boldsymbol{k},1}|\emptyset\rangle, \tag{7}$$

where $\psi^\dagger_{\boldsymbol{r},a}$ creates an electron on sublattice a in unit cell $\boldsymbol{r}$, $|\emptyset\rangle$ is the vacuum, $\psi^\dagger_{\boldsymbol{k},a}=(1/\sqrt{N})\sum_{\boldsymbol{r}}e^{i\boldsymbol{k}\cdot\boldsymbol{r}}\psi^\dagger_{\boldsymbol{r},a}$, and N is the total number of unit cells. The system is then time-evolved under an integer quantum Hall Hamiltonian $\hat{H}=\sum_{\boldsymbol{k}}\hat{H}(\boldsymbol{k})$, where $\hat{H}(\boldsymbol{k})=\sum_{a,b=1}^{N_B}H_{a,b}(\boldsymbol{k})\psi^\dagger_{\boldsymbol{k},a}\psi_{\boldsymbol{k},b}=\sum_{n=1}^{N_B}\epsilon_{\boldsymbol{k},n}\phi^\dagger_{\boldsymbol{k},n}\phi_{\boldsymbol{k},n}$, and we assume that the Chern number of all bands of $\hat{H}(\boldsymbol{k})$ are nonzero, $C_n\neq 0\ \forall n$. The overlap in Eq. (6) is $\langle\emptyset|\phi_{\boldsymbol{k},n}\psi^\dagger_{\boldsymbol{k},1}|\emptyset\rangle=\phi_1^{(n)}(\boldsymbol{k})^*$, where $\phi_a^{(n)}(\boldsymbol{k})=\langle a|\phi^{(n)}(\boldsymbol{k})\rangle$ is the ath component of $|\phi^{(n)}(\boldsymbol{k})\rangle=(\phi_1^{(n)}(\boldsymbol{k}),\phi_2^{(n)}(\boldsymbol{k}),\ldots,\phi_{N_B}^{(n)}(\boldsymbol{k}))^t$, an eigenvector of the postquench Hamiltonian matrix $H(\boldsymbol{k})$. It is known that any component $\phi_a^{(n)}(\boldsymbol{k})\ \forall a$ must have *at least* $|C_n|$ zeros in the Brillouin zone [46]; see also Theorem 1. Now assume that, at an arbitrary Bloch momentum $\boldsymbol{k}_0$, $\phi_1^{(n_1)}$ has the highest weight: $|\phi_1^{(n_1)}(\boldsymbol{k}_0)|>|\phi_1^{(n\neq n_1)}(\boldsymbol{k}_0)|$. The existence of a node means $\phi_1^{(n_1)}$ cannot remain as the highest weight element over the entire Brillouin zone and hence must switch rank with the second highest weight element—say, $\phi_1^{(n_2)}$—at some point $\boldsymbol{k}_c$: $|\phi_1^{(n_1)}(\boldsymbol{k}_c)|=|\phi_1^{(n_2)}(\boldsymbol{k}_c)|\geq|\phi_1^{(n\neq n_1,n_2)}(\boldsymbol{k}_c)|$ [47]. Together with the normalization $\langle\emptyset|\psi^\dagger_{\boldsymbol{k},1}\psi_{\boldsymbol{k},1}|\emptyset\rangle=\sum_n|\phi_1^{(n)}|^2=1$, one concludes that, at $\boldsymbol{k}=\boldsymbol{k}_c$, Eq. (6) is satisfied.

Note that, in this case, the return amplitude $G(\boldsymbol{k},t)$ is related to the $\boldsymbol{k}$-space sublattice particle density,

$$\rho_{\boldsymbol{k},a}(t)\equiv\langle\Psi(t)|\psi^\dagger_{\boldsymbol{k},a}\psi_{\boldsymbol{k},a}|\Psi(t)\rangle=|G(\boldsymbol{k},t)|^2. \tag{8}$$

A DQPT can thus be identified by $\rho_{\boldsymbol{k},a}(t^*)=0$, i.e., a complete depletion of particles with momentum $\boldsymbol{k}$ on sublattice a (or orbital, spin, etc.), which may be experimentally measurable.

The argument above for a node-protected DQPT applies to all pre- and postquench combinations. In general, if the overlap of the prequench band $|\psi(\boldsymbol{k})\rangle$ with *every* eigenstate $|\phi^{(n)}(\boldsymbol{k})\rangle$ of $H_F(\boldsymbol{k})$ has nodes in the Brillouin zone, then the triangle inequality Eq. (6) is guaranteed, and a robust DQPT would occur. This criterion can be written in a form more amenable to numerical testing,

$$\psi_{\text{MaxMin}}\equiv\max_n[\min_{\boldsymbol{k}}|\langle\phi^{(n)}(\boldsymbol{k})|\psi(\boldsymbol{k})\rangle|], \tag{9}$$

$$\psi_{\text{MaxMin}}=0\Leftrightarrow\text{Robust DQPT}. \tag{10}$$

Topological protection of nodes in wave function overlaps.—There is a curious connection between wave function zeros and quantization. In elementary quantum mechanics, nodes in the radial wave function is related to the principal quantum number [48]. In continuum integer quantum Hall systems, the number of nodes in the wave function $\psi(\boldsymbol{r})=\langle\boldsymbol{r}|\psi\rangle$ for $\boldsymbol{r}$ in a magnetic unit cell is given by its Chern number magnitude $|C|$ [46]. These nodes persist even in the presence of weak disorder [49]. On a lattice, $|C|$ gives the number of $\boldsymbol{k}$-space nodes in all wave function components $\psi_a(\boldsymbol{k})=\langle a|\psi(\boldsymbol{k})\rangle\ \forall a$ [46], a phenomenon closely related to the energetic spectral flow of the edge states [50]. Note that the relation between C and wave function nodes relies on one participant of the overlap —namely, the basis states $|\boldsymbol{r}\rangle$ and $|a\rangle$—to be topologically trivial. If both participants can be nontrivial, the number of nodes in their overlap should depend on both topological indices on an equal footing. Indeed, we have the following theorems.

Theorem 1.—In 2D, the overlap of Bloch bands $|\psi(\boldsymbol{k})\rangle$ and $|\phi(\boldsymbol{k})\rangle$, with Chern numbers C_ψ and C_ϕ, respectively, must have at least $|C_\psi-C_\phi|$ nodes in the Brillouin zone.

Theorem 2.—In 1D, the Berry phase γ of a real Bloch band, $|\psi(k)\rangle=(\psi_1(k),\psi_2(k),\cdots)^t$, $\psi_a(k)\in\mathbb{R}\ \forall a$ is quantized to 0 or π. The overlap of two real bands,

$|\psi(k)\rangle$ and $|\phi(k)\rangle$, with Berry phases γ_ψ and γ_ϕ, respectively, must have at least one node if $\gamma_\psi \neq \gamma_\phi$. See the SM [43] for a proof. Note that symmetry protection may enforce a Hamiltonian to be real [51], leading to the real bands in Theorem 2. This prompts the notion of symmetry-protected DQPT, reminiscent of symmetry-protected topological phases that may be classified by topological numbers at high-symmetry hypersurfaces [51–53]. An example will be given later; see also the SM [43].

Generalized Hofstadter model.—We demonstrate ideas discussed above using a generalized Hofstadter model,

$$H(\boldsymbol{k},t,m) = \begin{pmatrix} d_1 & v_1 & v_3 e^{ik_y} \\ v_1 & d_2 & v_2 \\ v_3 e^{-ik_y} & v_2 & d_3 \end{pmatrix},$$
$$d_a = 2\cos(k_x + a\varphi) + am,$$
$$v_a = 1 + 2t\cos\left[k_x + \left(a + \frac{1}{2}\right)\varphi\right],$$
$$a = 1,2,3, \varphi = \frac{2\pi}{3}. \tag{11}$$

The nearest neighbor hopping is set at 1. At $t = m = 0$, we recover the Hofstadter model [50,54–59] on a square lattice with a magnetic flux φ per structural unit cell, and its magnetic unit cell consists of three structural unit cells along the y direction. $t \neq 0$ allows for second neighbor (i.e., diagonal) hopping, and $m \neq 0$ describes a flux-commensurate on-site sawtooth potential. See the SM [43] for a phase diagram. At $k_y = 0$ and π, $H(\boldsymbol{k})$ is invariant under the combined transformation of time reversal, $H(\boldsymbol{k}) \to H^*(-\boldsymbol{k})$, and inversion, $H(\boldsymbol{k}) \to H(-\boldsymbol{k})$, and hence is real. Eigenstates there are subject to Theorem 2.

Now consider quenches in which the initial state is prepared by filling one of the three bands of a prequench Hamiltonian parametrized by t_i, m_i and evolved using a postquench Hamiltonian with t_f, m_f [60]. In Fig. 2, we keep t_i, m_i, m_f fixed, and plot ψ_{MaxMin}, as defined in [Eq. (9)] of the three prequench bands as functions of the postquench t_f. By varying t_f, the postquench $H(\boldsymbol{k})$ is swept through six different topological phases, as labeled in Fig. 2.

Let us illustrate topological and symmetry-protected DQPTs with two examples, using $\psi^{(2)}$ as the prequench state (the green squared line in Fig. 2). (i) *Topological DQPT protected by a 2D Chern number.*— Consider the quench from $\psi^{(2)}$ to phase 5. In this case, the Chern number of the prequench state ($C = -1$) differs from *all three* Chern numbers of the postquench Hamiltonian ($C = [1, -2, 1]$); thus, from Theorem 1, all three overlaps have nodes, and Eq. (6) is satisfied. (ii) *Symmetry-protected DQPT.*— Consider the quench from $\psi^{(2)}$ to phase 2. In this case, the prequench Chern number ($C = -1$) is identical to at least one of the postquench Chern numbers ($C = [0, 1, -1]$); hence, not all overlaps have nodes

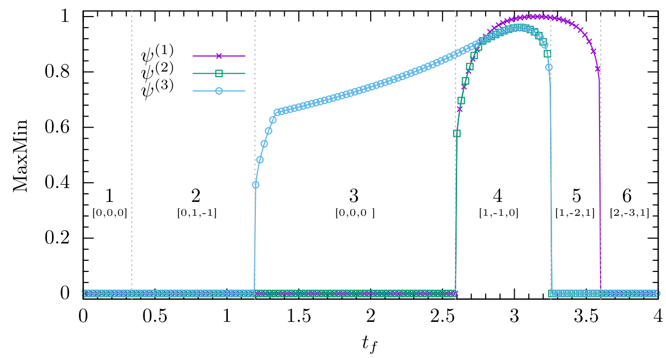

FIG. 2. Plot of ψ_{MaxMin} [Eq. (9)] as functions of the postquench t. The prequench state is prepared by filling one of the three bands $\psi^{(1,2,3)}$ of the generalized Hofstadter model Eq. (11) with parameters $t_i = 3$ and $m_i = 2.8$. Postquench $H(\boldsymbol{k})$ has fixed $m_f = 3$ and a varying t_f, sweeping it through six topological phases labeled by its three Chern numbers (ordered from the lower to the higher band). The prequench Hamiltonian is in phase 4. A robust DQPT can be identified by $\psi_{\mathrm{MaxMin}} = 0$ [Eq. (10)]. Note that ψ_{MaxMin} changes between zero and nonzero only at phase boundaries, verifying robust DQPT as a feature of topological phases insensitive to parameter tuning. See the SM [43] for a detailed account of all 18 types of quenches shown here.

originating from Theorem 1. Nevertheless, at $k_y = 0$ and π, where the Hamiltonian is real, its eigenstates can be classified by their Berry phases. One can find numerically that, at $k_y = 0$, the Berry phase for $\psi^{(2)}$ is $\gamma = 0$, whereas that of the postquench $\phi^{(3)}$ (the one with $C = -1$) is $\gamma = \pi$. According to Theorem 2, therefore, $\langle\phi^{(3)}|\psi^{(2)}\rangle_{k_y=0}(k_x)$ has a node along k_x. Nodes in overlaps of $\psi^{(2)}$ with $\phi^{(1)}$ and $\phi^{(2)}$ are still protected by Theorem 1. Thus, all three overlaps have nodes and the DQPT is protected.

Details of all 18 quench types (three prequench states × six postquench phases) can be found in the SM [43]. We should note here that out of all 18 types, two robust DQPTs ($\psi^{(1)}$ to phases 2 and 5) exhibit an even number of overlap nodes at $k_y = 0$ and/or π not accounted for by Theorems 1 and 2. By tuning $t_{i,f}$ and $m_{i,f}$, we were able to shift the nodes along k_x as well as to change the total number of nodes by an even number, but we could not entirely eliminate them. We suspect, however, that they could eventually be eliminated in an enlarged parameter space.

Conclusion and discussion.—In this Letter, we showed that, for quantum quenches between gapped phases in a generic multiband system, a robust DQPT is a consequence of momentum-space nodes (or zeros) in the wave function overlap between the prequench state and all postquench energy eigenstates. Nodes in wave function overlaps are topologically protected if the topological indices of the two participating wave functions—such as the Chern number in 2D and the Berry phase in 1D—are different.

Our main tenets here are the triangle inequality equation (6), and the phase ergodicity. It is interesting to note that collapsing a band gap would affect both conditions: right at the gap collapsing point $\varepsilon_{\mathbf{k}}^{(n)} = \varepsilon_{\mathbf{k}}^{(n+1)}$, the two phases become mutually locked; as the gap reopens, the system has gone through a topological transition, which changes the node structure in wave function overlaps. We also note that while the *existence* of a topological and symmetry-protected DQPT is insensitive to details of the energy band structure, the exact times at which it would occur will inevitably depend on the latter. The shortest critical time will be upper bounded by the recurrence time of the phases, which, for few-level systems such as band insulators, should remain physically relevant [61].

The DQPT in band systems is, in principle, experimentally measurable. As shown in Eq. (8), the DQPT can be identified as the depletion of sublattice particle density $\rho_{\mathbf{k},a}(t^*)$, where sublattice a can also refer to the spin, the orbital, etc. Particle density $\rho_{\mathbf{k}}(t) = \sum_a \rho_{\mathbf{k},a}(t)$ can already be measured in cold atom systems by time-of-flight experiments [1–3,55,63]. It is not hard to envisage an additional procedure of sublattice isolation in such measurements, e.g., by using a magnetic field for spin filtering, or by releasing other sublattices $b \neq a$ slightly earlier than a.

We are grateful to D. P. Arovas, A. Alexandradinata, and A. Saxena for the useful discussions. We thank J. M. Zhang for communications regarding a recent work [62]. Work at LANL was supported by U.S. DOE Grant No. BES E304/E3B7. Work at NORDITA was supported by ERC Grant No. DM 321031.

Note added in proof.—Recently, Ref. [64] appeared shortly after the completion of this manuscript, where results regarding topological nodes in wave function overlaps, consistent with Theorems 1 and 2 presented here, are obtained elegantly by appealing to adiabatic continuity. In Ref. [65], topological nodes have also been connected to non-analyticity in physical observables upon tuning the postquench Hamiltonian across a topological transition. We thank K. Sun and A. Das for communications.

*zsh@lanl.gov
†avb@nordita.org

[1] I. Bloch, J. Dalibard, and W. Zwerger, Rev. Mod. Phys. **80**, 885 (2008).
[2] I. Bloch, J. Dalibard, and S. Nascimbène, Nat. Phys. **8**, 267 (2012).
[3] T. Langen, R. Geiger, and J. Schmiedmayer, Annu. Rev. Condens. Matter Phys. **6**, 201 (2015).
[4] A. Polkovnikov, K. Sengupta, A. Silva, and M. Vengalattore, Rev. Mod. Phys. **83**, 863 (2011).
[5] F. Iglói and H. Rieger, Phys. Rev. Lett. **85**, 3233 (2000).
[6] E. Altman and A. Auerbach, Phys. Rev. Lett. **89**, 250404 (2002).
[7] A. Polkovnikov, S. Sachdev, and S. M. Girvin, Phys. Rev. A **66**, 053607 (2002).
[8] K. Sengupta, S. Powell, and S. Sachdev, Phys. Rev. A **69**, 053616 (2004).
[9] P. Calabrese and J. Cardy, Phys. Rev. Lett. **96**, 136801 (2006).
[10] R. Barankov and A. Polkovnikov, Phys. Rev. Lett. **101**, 076801 (2008).
[11] F. Pollmann, S. Mukerjee, A. G. Green, and J. E. Moore, Phys. Rev. E **81**, 020101 (2010).
[12] R. Nandkishore and D. A. Huse Annu. Rev. Condens. Matter Phys. **6**, 15 (2015).
[13] J. Eisert, M. Friesdorf, and C. Gogolin, Nat. Phys. **11**, 124 (2015).
[14] L. D'Alessio, Y. Kafri, A. Polkovnikov, and M. Rigol, Adv. Phys.**65**, 239 (2016).
[15] F. H. L. Essler and M. Fagotti, J. Stat. Mech. (2016) 064002.
[16] J. Millen and A. Xuereb, New J. Phys. **18**, 011002 (2016).
[17] A. LeClair, G. Mussardo, H. Saleur, and S. Skorik, Nucl. Phys. **B453**, 581 (1995).
[18] M. Heyl, A. Polkovnikov, and S. Kehrein, Phys. Rev. Lett. **110**, 135704 (2013).
[19] M. Fagotti, arXiv:1308.0277.
[20] M. E. Fisher, The Nature of Critical Points, *Lectures in Theoretical Physics* Vol. 7 (University of Colorado Press, Boulder, CO, 1965).
[21] C. N. Yang and T. D. Lee, Phys. Rev. **87**, 404 (1952); T. D. Lee and C. N. Yang, Phys. Rev. **87**, 410 (1952).
[22] The formal similarity between e^{-iHt} and $e^{-\beta H}$ is routinely used in field theoretic calculations such as correlators, where the thermal and quantum-dynamic results are related through Wick rotation. Knowledge in one domain can then be transcribed into the other without additional calculation. This "equivalence," however, relies on the existence of an analytic continuation between it and β in the complex temperature plane. The presence of closed and/or semi-infinite Fisher zero lines divides the complex temperature plane into disjoint regions, and the correspondence between it and β will break down if they reside in different regions. For quenches that exhibit a DQPT, as pointed out in Ref. [18] this implies that nonequilibrium time evolution (i.e., along the imaginary temperature axis) is, in general, not governed by the equilibrium thermodynamics (along the real temperature axis).
[23] B. Pozsgay, J. Stat. Mech. (2013) P10028.
[24] S. Vajna and B. Dóra, Phys. Rev. B **89**, 161105 (2014).
[25] J. M. Hickey, S. Genway, and J. P. Garrahan, Phys. Rev. B **89**, 054301 (2014).
[26] S. Vajna and B. Dóra, Phys. Rev. B **91**, 155127 (2015).
[27] M. Schmitt and S. Kehrein, Phys. Rev. B **92**, 075114 (2015).
[28] U. Divakaran, S. Sharma, and A. Dutta, Phys. Rev. E **93**, 052133 (2016).
[29] S. Sharma, U. Divakaran, A. Polkovnikov, and A. Dutta, Phys. Rev. B **93**, 144306 (2016).
[30] J. C. Budich and M. Heyl, Phys. Rev. B **93**, 085416 (2016).
[31] C. Karrasch and D. Schuricht, Phys. Rev. B **87**, 195104 (2013).
[32] J. N. Kriel, C. Karrasch, and S. Kehrein, Phys. Rev. B **90**, 125106 (2014).
[33] F. Andraschko and J. Sirker, Phys. Rev. B **89**, 125120 (2014).

[34] S. Sharma, S. Suzuki, and A. Dutta, Phys. Rev. B **92**, 104306 (2015).
[35] E. Canovi, P. Werner, and M. Eckstein, Phys. Rev. Lett. **113**, 265702 (2014).
[36] M. Heyl, Phys. Rev. Lett. **115**, 140602 (2015).
[37] P. Talkner, E. Lutz, and P. Hänggi, Phys. Rev. E, **75**, 050102 (R) (2007).
[38] M. Campisi, P. Hänggi, and P. Talkner, Rev. Mod. Phys. **83**, 771 (2011); **83**, 1653(E) (2011).
[39] C. Jarzynski, Phys. Rev. Lett. **78**, 2690 (1997).
[40] S. Deffner and A. Saxena, Phys. Rev. E **92**, 032137 (2015).
[41] M. Heyl, Phys. Rev. Lett. **113**, 205701 (2014).
[42] For example, in 2D integer quantum Hall systems, the DQPT is related to the change in the absolute value of Chern number $|C|$ instead of C [26].
[43] See Supplemental Material at http://link.aps.org/supplemental/10.1103/PhysRevLett.117.086802 for proofs of theorems and detailed analysis of models.
[44] A. Kitaev, Ann. Phys. (Amsterdam) **321**, 2 (2006).
[45] I. Cornfeld, A. Sossinskii, S. Fomin, and Y. Sinai, *Ergodic Theory* (Springer, New York, 1982).
[46] M. Kohmoto, Ann. Phys. (N.Y.) **160**, 343 (1985).
[47] For two-band models, $\boldsymbol{k}_c$ is where the so-called population inversion occurs.
[48] L. D. Landau and E. M. Lifshits, *Quantum Mechanics: Non-relativistic Theory* (Butterworth-Heinemann, Oxford, 1977).
[49] D. P. Arovas, R. N. Bhatt, F. D. M. Haldane, P. B. Littlewood, and R. Rammal, Phys. Rev. Lett. **60**, 619 (1988).
[50] Y. Hatsugai, Phys. Rev. Lett. **71**, 3697 (1993).
[51] C. Fang, Y. Chen, H.-Y. Kee, and L. Fu, Phys. Rev. B **92**, 081201 (2015).
[52] S. Ryu, A. P. Schnyder, A. Furusaki, and A. W. W. Ludwig, New J. Phys. **12**, 065010 (2010).
[53] A. Alexandradinata, C. Fang, M. J. Gilbert, and B. A. Bernevig, Phys. Rev. Lett. **113**, 116403 (2014).
[54] D. R. Hofstadter, Phys. Rev. B **14**, 2239 (1976).
[55] E. Zhao, N. Bray-Ali, C. J. Williams, I. B. Spielman, and I. I. Satija, Phys. Rev. A **84**, 063629 (2011).
[56] Z. Huang and D. P. Arovas, Phys. Rev. B **86**, 245109 (2012).
[57] L. Wang, A. A. Soluyanov, and M. Troyer, Phys. Rev. Lett. **110**, 166802 (2013).
[58] F. Harper, S. H. Simon, and R. Roy, Phys. Rev. B **90**, 075104 (2014).
[59] M. Aidelsburger, M. Lohse, C. Schweizer, M. Atala, J. T. Barreiro, S. Nascimbène, N. R. Cooper, I. Bloch, and N. Goldman, Nat. Phys. **11**, 162 (2015).
[60] An initial state of two filled bands is equivalent to one with a single filled band through a particle-hole transformation.
[61] Under special circumstances, the DQPT critical time may also emerge at a much shorter time scale, e.g., the inverse level spacing; see Ref. [62].
[62] J. M. Zhang and H.-T. Yang, Europhys. Lett. **114**, 60001 (2016).
[63] D.-L. Deng, S.-T. Wang, and L.-M. Duan, Phys. Rev. A **90**, 041601 (2014).
[64] J. Gu and K. Sun, arXiv:1605.07627.
[65] S. Roy, R. Moessner, and A. Das, arXiv:1606.06673.